Available online at www.sciencedirect.com

SciVerse ScienceDirect

Journal of the European Ceramic Society 32 (2012) 371–379

www.elsevier.com/locate/jeurceramsoc

Original article

Cordierite synthesis. A time-resolved neutron diffraction study

J.M. Benito [a], X. Turrillas [b], G.J. Cuello [c], A.H. De Aza [a], S. De Aza [a], M.A. Rodríguez [a,*]

[a] *Instituto de Cerámica y Vidrio, CSIC, C/ Kelsen 5, 28049 Madrid, Spain*
[b] *Centro de Seguridad, Durabilidad Estructural y de Materiales (CISDEM), CSIC, C/Serrano Galvache 4, 28033 Madrid, Spain*
[c] *Institute Laue Langevin (ILL), 6, rue Jules Horowitz, BP 156, F-38042 Grenoble Cedex 9, France*

Received 24 March 2011; received in revised form 31 August 2011; accepted 12 September 2011
Available online 10 October 2011

Abstract

In order to elucidate the mechanism of reaction during the cordierite synthesis a kinetic study has been carried out by means of X-ray diffraction and neutron thermo-diffraction. It was thus possible to elucidate between the reactions leading to the cordierite synthesis and those that gave rise to the undesired phases generated during this process. Depending on the reactants used these reactions are different. The present paper presents results obtained during the cordierite synthesis starting from talc, kaolin and hydromagnesite as reactants. This synthesis from natural raw materials takes place through a complex mechanism that has been described. In this kind of synthesis, at the end of the entire process the obtained cordierite is always accompanied by a second phase: spinel. This is the first time that the presence of the μ-cordierite phase has been observed when the synthesis is carried out in solid state from non-submicronic natural raw materials.

Keywords: Powders-solid state reaction; X-ray methods; Cordierite

1. Introduction

The cordierite ($2MgO{\cdot}2Al_2O_3{\cdot}5SiO_2$) is one of the ternary compounds within the $MgO–Al_2O_3–SiO_2$ system (Fig. 1). It melts incongruently at 1465 °C producing mullite and a liquid [1]. Cordierite based materials have a great importance in modern technology due to their excellent properties: low thermal expansion coefficient, high refractoriness, low dielectric constant, high thermal shock resistance and good mechanical properties. Keeping in mind all these properties, nowadays these materials are used as support of catalysts in the car industry, as refractory material (fast cycle furnaces, metal coatings), heat exchangers, substrates in microelectronic, supports of membranes, gas burners, etc. [2].

The cordierite is characterized by a complex polymorphism [3,4]:

- The α-cordierite, of hexagonal symmetry (also well-known as indialite [5]), takes place by a quick crystallization between 1000 and 1300 °C.
- The β-cordierite, of orthorhombic structure, is obtained by crystallization below 950 °C. This is the most common phase in natural cordierite [5].
- The μ-cordierite, metaestable rhombohedral phase is obtained by the crystallization of cordierite glass below 925 °C. This phase is also known just as an aluminum magnesium silicate [6].

At 800 °C the first phase that crystallizes, in the submicronic particle size range, is the μ-cordierite. Later on, at temperatures close to 800, this phase becomes the β phase, the most stable polymorph. With the temperature rising, the forms β and μ pass to α phase (indialite), with a great volume increase, but only above 1450 °C, this phase remains stable [7]. The μ-cordierite can also transform directly to the α phase by heating at 980 °C during 2 h as reported elsewhere [8]. Below 1450 °C the α phase slowly transforms into the β phase accompanied by a structural rearrangement [8].

One of the ways to distinguish α and β phases is by means of X-ray diffraction (XRD), because using the CuKα radiation at least 3 peaks of β-cordierite appear in 2θ ranging 29° and 30°, while only one peak is observed for the α phase [5,9]. However, when a mixture of several polymorphic phases exists, these 3 peaks appear as one making very difficult to clearly

* Corresponding author.
E-mail address: mar@icv.csic.es (M.A. Rodríguez).

0955-2219/$ – see front matter © 2011 Elsevier Ltd. All rights reserved.
doi:10.1016/j.jeurceramsoc.2011.09.010

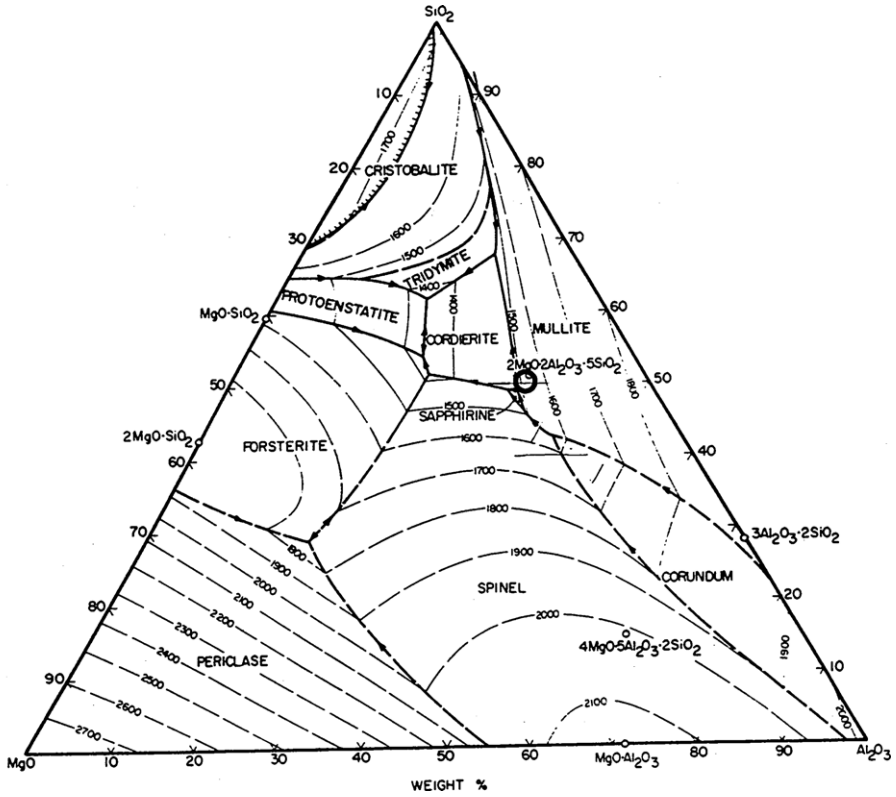

Fig. 1. $MgO–Al_2O_3–SiO_2$ Phase Equilibrium Diagram [1]. (◯) Stoichiometric composition.

discern whether only α cordierite is present or there is an α–β cordierite mixture [5].

With no doubts the best method to discern among the different structures is by means of Nuclear Magnetic Resonance [7,10].

One of the main problems of the cordierite is its small field of existence due to the vicinity of 6 invariant points (Fig. 1 and Table 1). Small variations with regard to the stoichiometric composition can generate non-desired secondary reactions.

For this reason it is easy to find the cordierite with secondary phases as mullite, corundum, spinel, forsterite, clinoenstatite and cristobalite. De Aza et al. [11] concluded that in any process of cordierite synthesis it is difficult to predict the compounds that will be obtained, since the relationship among phases depends on temperature, on time as well as on mechano-chemical activation [12].

Table 1
Invariant points that surround the primary field of the cordierite.

Temperature (°C)	Type	Phases
1355	Eutectic	Protoenstatite–tridimite–cordierite
1440	Peritectic	Tridimite–mullite–cordierite
1460	Peritectic	Mullite–saphirine–cordierite
1453	Peritectic	Saphirine–spinel–cordierite
1370	Peritectic	Spinel–forsterite–cordierite
1365	Eutectic	Forsterite–protoensatite–cordierite

Nowadays, from an industrial point of view, the cordierite is commonly synthesized by reaction among kaolin, talc and some compound that supplies the magnesium, or also by reaction among of kaolin, talc or alumina [13]. At laboratory scale another type of mixtures are also used, as those formed by talc, alumina and wastes coming from the coal combustion [14], talc, kieselguhr and alumina [15], talc, fused silica and wastes of the coal combustion [16], rice husk and silica [17], sepiolite, kaolin and quartz or feldspar, kaolin, talc and silica [18], or also by sol–gel process [16,19].

The main objective of the present study is to determine the mechanism of reaction during cordierite synthesis. So far its formation mechanism has only been explained on hypothetical basis [17,20], but do not exist clear experimental studies confirming these hypotheses. In order to elucidate the exact mechanism of synthesis, an experimental study has been carried out by means of XRD and Neutron thermo-diffraction. For instance, *in situ* time-resolved neutron diffraction (TRND) has been useful in monitoring the decomposition of dolomite while heating [21] or studying the synthesis mechanism of NiAl based materials by thermal explosion method [22]. It was thus possible to elucidate between the reactions leading to the cordierite synthesis and those that gave rise to the undesired phases generated during this process. Moreover, these reactions are different depending on the reactants used. For the sake of brevity, the present paper only presents results obtained during the cordierite synthesis starting from talc, kaolin and hydromagnesite as reactants.

2. Materials and methods

2.1. Raw materials and sample preparation

The composition studied in this work has been formulated in order to obtain stoichiometric cordierite, that is: 34.8% of Al_2O_3, 51.4% of SiO_2 and 13.8% of MgO, in weight (Fig. 1) starting from raw materials: talc, kaolin and hydromagnesite as reactants.

High purity starting materials have been chosen in order to avoid, as much as possible, the formation of non-wanted compounds through secondary reactions. Those used have been:

- $2SiO_2{\cdot}Al_2O_3{\cdot}2H_2O$ (Kaolin, Type E. Caobar SA, Spain). See Table 3 for details.
- $Mg_3(Si_4O_{10})(OH)_2$ (Talc, P Especial, Boñar SA, Spain). See Table 4 for details.
- $Mg_5(CO_3)_4(OH)_2(H_2O)_4$ (magnesium hydroxicarbonate, Merck, Germany), purity > 99% (hydromagnesite).

The preparation of the studied samples has been carried out mixing the appropriate quantities of each material, during 1 h in an attrition mill, with high purity alumina balls in a 1:1 (volume) ratio. The mixture was carried out with isopropyl alcohol as liquid media. Later on, the samples were dried at 60 °C ensuring the complete evaporation of the alcohol.

Two kinds of experiments have been carried out. *Static experiments*, where the samples were heated in an electric furnace up to different temperatures (with heating rates of 5 °C/min) and characterized after cooling and *Dynamics experiments* where the samples were heated in a special furnace and simultaneously the changes on the samples were followed and registered by means of Neutron diffraction experiments.

Static experiments have been performed at 1000 °C, 1100 °C, 1200 °C and 1300 °C with dwell time of 30 min. Samples have been quenched with a cold air flow. The samples for these experiments have been uniaxially pressed at 125 MPa in a cylindrical shape (8 mm in diameter and 5 mm in height). After the thermal treatments, the samples obtained were milled to a size <63 μm for the XRD study.

Thermal analysis (DTA, TG), XRD and chemical analysis of the raw materials have been also carried out, when it was considered necessary, in order to a better understanding of the mechanism. Particle size by laser scattering and specific surface by Nitrogen adsorption measurements were carried out to elucidate some parameters that could have influenced on the kinetic.

2.2. Characterization

Particle size analysis was carried out with a Mastersizer Laser Analyser (Malvern, UK), and for the specific surface a Monosorb Surface Area Analyzer, model MS-13 (Quantachrome Corporation, US) was used.

Chemical Analysis of Kaolin and Talc (SiO_2, Al_2O_3) was carried out by X-ray fluorescence, using Philips spectrometer model MagiX Super Q Version 3.0 (The Netherlands) and the thermal analysis was carried out in a Netzst Simultaneous Thermal Analysis mod. STA 409 (Germany).

For the XRD diffraction pattern, recording of the data was made with powdered sample running on a Siemens Diffractometer D5000 (Germany) using Cu Kα radiation (λ = 1.54056 Å). Acquisition was made in the 2θ range of 20° to 80° with a step of 0.03° and 5 s of integration time per step.

2.3. Neutron thermo-diffraction

In the second type of experiments (dynamic ones), the real time evolution of the different compositions with the temperature has been carried out by neutron thermo-diffraction.

The neutron diffraction (ND) is based in the same principle of the XRD, however the interaction of the neutrons with the matter is different. In the case of X-rays, the photons interact with the electron cloud of the atoms, while the neutrons (without electrical charge), interact directly with the nuclei of the material without interacting with electrons. As consequence they can cross thickness of several centimeters without significant losses of intensity. This is the main difference with XRD and thanks to this ND presents certain advantages for this kind of studies [23,24].

This study has been carried out at the Institute Max Von Laue – Paul Langevin (ILL) (Grenoble, France), operating a nuclear reactor with a fuel element of about 1 m of diameter and a thermal power of 58 MW and a flux of neutrons of 1.5×10^{15} n cm^{-2} s^{-1}.

The instrument used was a powder diffractometer (D1B line) that uses thermal neutrons. This equipment has two monochromators (germanium and pyrolytic graphite) that allow selecting wavelengths of 1.28 and 2.52 Å respectively. The system is equipped with a multichannel detector composed by 400 cells that covers an angular range of 80°, ranging 2° to 160° if the detector is displaced.

In order to improve the reaction of the starting materials during the dynamic experiments, the samples for these experiments have been mixing by an attrition mill and they were subsequently compacted by cold isostatic pressing using a NFE press (National Forge Europe – Belgium) up to a pressure of 50 MPa to obtain samples approximately with cylindrical form of 8 mm in diameter.

These samples were introduced in an approximately cylindrical niobium holder with 80 mm in length and 10 mm in diameter, which in turn was fixed into the furnace.

The *in situ* study of the formation mechanism of the cordierite has been carried out using a neutron wavelength of 2.5145 Å. The time of acquisition was of 150 s, the angular step of 0.2° and the angular interval between 10° and 90°.

The experiments were carried out using a high temperature furnace placed on the way of neutrons beam. The temperature control was carried out using two Pt–Rh thermocouples, one within the furnace (thermocouple for furnace control) and the other one in contact with the sample (thermocouple for reaction temperature measure). The heating rate was of 300 °C h^{-1} up to 1300 °C.

The neutron diffraction data collected during the heating cycle were represented as a sequence of patterns in a pseudo-three-dimensional fashion in which the x-axis corresponds to the diffraction angle 2θ, the y-axis to the temperature, and the z-axis to the relative intensity (Fig. 8). To visualize events such as diffraction line shifts or growth and collapse of phases more precisely, a contour map in two dimensions was also projected from the 3D plot (Fig. 7). The existence of phase domains is clearly highlighted by their diffraction peaks shown in the figure as contour lines. Software routines developed at ILL were used in order to carry out the integration of the intensity of the reflections. Neutron diffraction data were conditioned and reflection peaks fitted to Gaussian with the help of code written in IDL [25].

3. Results and discussion

The characterization of the raw materials was carried out as a first step with the aim of a better analysis of the behavior of the reactive mixture.

3.1. Raw materials characterization

In Table 2 the mean particle size and the specific surface values obtained for the starting materials are shown.

The rational analysis of the kaolin is shown in the Table 3, together with the chemical analysis when it has been heated at 1000 °C and the theoretical composition of kaolinite (in oxide form). As it can be appreciated it is formed basically of SiO_2 and Al_2O_3, and their percentages are adjusted very well to those corresponding to pure kaolinite.

Through XRD it has been clearly determined the kaolinite and quartz presence in the raw material (Fig. 2). In order to observe the presence of certain impurities that they can go with the kaolinite (like occurs in micas), the diffraction pattern of the kaolin was also obtained in the oriented aggregates way. For this a drop of kaolin dispersion was deposited on a slide and dried. Considering the diffraction pattern obtained,

Table 2
Morphological characterization of the starting materials used.

	Mean particle size (μm)	Specific surface ($m^2\ g^{-1}$)
Talc	17.3 ± 0.7	4.4 ± 0.2
Kaolin	5.6 ± 0.1	8.5 ± 0.4
Hydromagnesite	42.6 ± 0.2	11.2 ± 0.6

Table 3
Rational analysis of the kaolin used in this study.

	Kaolin (% weight)	Calcined kaolin (% weight)	Kaolinite (% theoretical)
Loss of ignition (1000 °C)	13.02	–	13.95
SiO_2	48	56	46.55
Al_2O_3	37	43	39.50
TiO_2, Fe_2O_3, MgO, CaO, Na_2O, K_2O	<2	≈1	

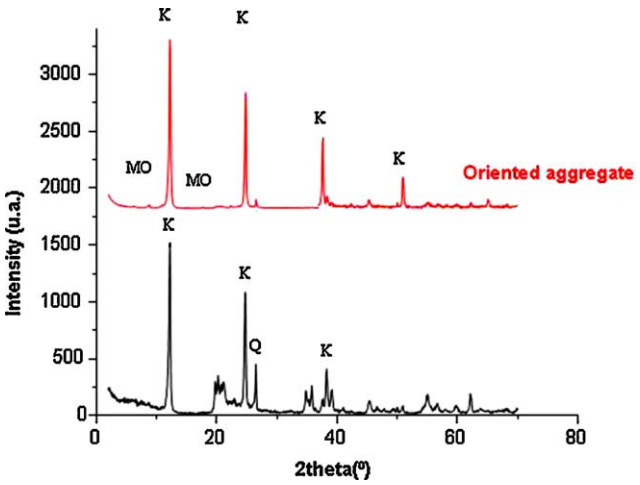

Fig. 2. Standard XRD pattern and oriented aggregate XRD pattern of the used kaolin. K – kaolinite, Q – α-quartz and MO – muscovite.

it can be concluded the existence of 3 compounds, kaolinite ($2SiO_2{\cdot}Al_2O_3{\cdot}2H_2O$), a small amount of quartz (α-SiO_2) and muscovite ($KAl_2(Si_3Al)O_{10}{\cdot}(OH)_2$). These results allow the evaluation of the proportion of these compounds in the starting material as, approximately, 90% kaolinite, 5% quartz and 5% muscovite.

The thermal analysis of the kaolin shows an endothermic effect located at 550 °C corresponding to 13% of loss of weight. This process corresponds to the dehydration of the kaolinite to meta-kaolin (a well-known process not shown in this paper).

Table 4 shows the rational analysis of the talc ($3MgO{\cdot}4SiO_2{\cdot}H_2O$). These results show that the percentages of SiO_2 and of MgO correspond quite well with stoichiometric talc, for that is not expected the existence of high percentages of other phases.

The loss of ignition is higher than that corresponding to talc, showing the presence of some type of impurity with a clear loss of weight.

Analyzing their corresponding diffraction pattern (Fig. 3), it can be observed that it is fundamentally formed by talc, small amounts of quartz and of dolomite ($CaMg(CO_3)_2$). These "impurities" are commonly associated to the talc, as mentioned by other authors [26].

It has been estimated that this starting material is composed by 2% dolomite, 97% of talc and 1% quartz.

The hydromagnesite used as raw material for this study possesses a purity bigger than 99%, making unnecessary the corresponding chemical analysis. Fig. 4 shows the diffraction pattern of this compound of chemical formula

Table 4
Rational analysis of the talc used in this study.

	Talc (% weight)	Talc (% theoretical)
Loss of ignition (1000 °C)	5.72	4.75
SiO_2	62	63.35
MgO	32	31.90
CaO, Fe_2O_3, TiO_2, Al_2O_3, Na_2O, K_2O	<1	

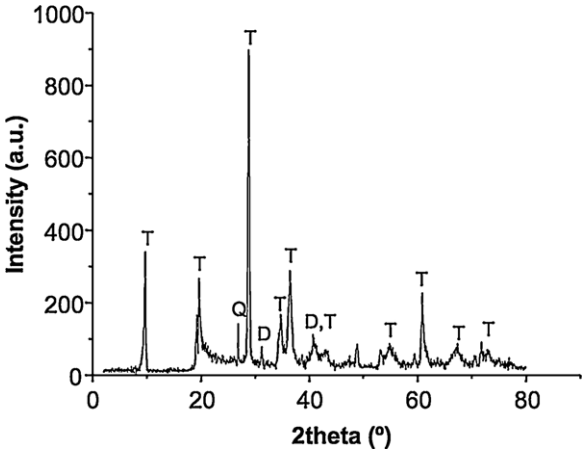

Fig. 3. XRD pattern of talc. T – talc, Q – α-quartz and D – dolomite.

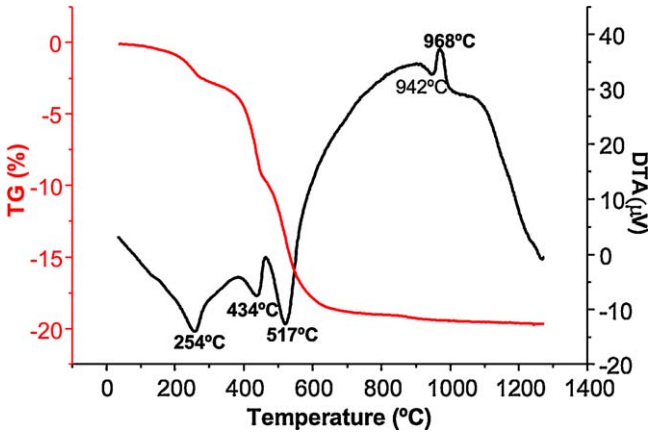

Fig. 5. DTA-TG analysis of the Stoichiometric composition prepared to obtain cordierite. Heating rate 120 °C h^{-1}.

$Mg_5(CO_3)_4(OH)_2{\cdot}4H_2O$ [27,28], where the most intense peaks have been pointed out, nevertheless it is necessary to point out that all the peaks present correspond to this phase.

The composition, in order to obtain the cordierite, could be formulated as 7.13% talc, 76.06% kaolin and 16.81% hydromagnesite, taking into account the results of reactants characterization.

3.2. Composition study

The DTA analysis of the composition (Fig. 5) shows 3 endothermic effects accompanied by a loss of weight. The first of them (whose maximum is at 254 °C) is due to the loss of the crystallization water of the hydromagnesite. The process centered at 434 °C would also correspond to the loss of the OH groups of the hydromagnesite. And finally, the endothermic process at 517 °C corresponds to the decarbonation of the hydromagnesite and the dehydroxilation of the kaolinite, both jointly.

At 942 °C it can observe the endothermic effect corresponding to the decomposition of the talc. The associated mass loss is not appreciated clearly due to the low percentage of talc in the composition. At 968 °C an exothermic effect is observed associated to the coordination change of the Al in the metakaolinite.

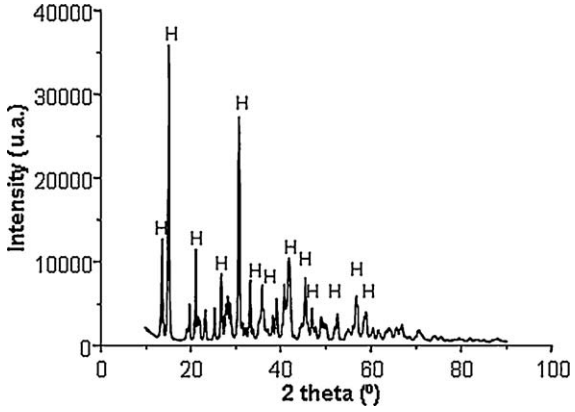

Fig. 4. XRD pattern of Hydromagnesite (H).

The total loss of mass taken place up to 1200 °C is approximately of 20%.

The evolution of this decomposition through XRD at different temperatures is shown in Fig. 6.

According to the thermogravimetric study of this decomposition (Fig. 5), at 1000 °C the decomposition of all the starting materials has taken place. For this reason in the corresponding diffraction pattern (Fig. 6) any rest is observed neither of talc, neither of kaolinite, neither of the hydromagnesite. Nevertheless the products of their decomposition, enstatite, mullite (in very low proportion) and periclase are observed. The silica, coming from the decomposition of the kaolinite and talc, has not been detected due to their low crystallinity, but remaining quartz and the presence of μ-cordierite and spinel ($MgO{\cdot}Al_2O_3$) can be observed. The mentioned quartz was an impurity in the kaolin and the talc, and concretely it corresponds to α-quartz that is stable at room temperature [29]. μ-Cordierite and spinel are compounds that have been generated by some specific reaction to be determined later on.

At 1100 °C the amount of all the phases observed at 1000 °C increases, with the exception of quartz, μ-cordierite and periclase. The quartz peaks keep a similar intensity, indicating that this compound has not suffered any reaction or transformation process. However with regard to the μ-cordierite, this has disappeared in the change of temperature from 1000 to 1100 °C. Also it can be observed that the periclase peaks have decreased in intensity.

The tendency observed at 1100 °C also remains at 1200 °C, that is the mullite and enstatite proportion is increased in the mixture. At this temperature it can be also appreciated the cristobalite appearance. Analyzing this diffraction pattern, some peaks corresponding to the cordierite are already observed, however they have not been indicated because this formation is not completely evident.

Finally at 1300 °C, it can be observed the formation of the cordierite and, as impurities some percentages of mullite, cristobalite and spinel have also been obtained. Analyzing the formed cordierite using the method described by Miyashiro [5,9] it can be deduced that the obtained phase is the low temperature one.

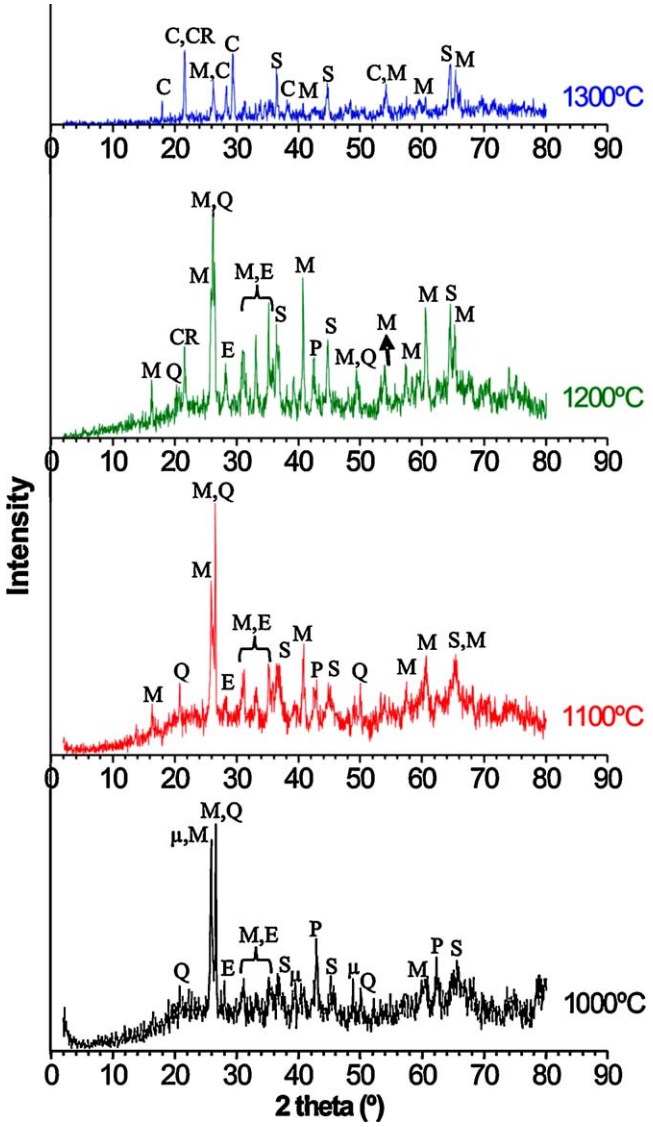

Fig. 6. Phase's evolution of the studied composition. XRD patterns. Q – α-quartz, μ – μ-cordierite, M – mullite, E – enstatite, S – spinel, P – periclase, CR – cristobalite, C – β-cordierite.

Also it can be observed that the enstatite and the quartz have disappeared.

3.2.1. Neutron thermodiffraction

As mentioned previously, the neutron diffraction data collected during the heating cycle were represented as a sequence of patterns in a pseudo-three-dimensional fashion in which the *x*-axis corresponds to the diffraction angle 2θ, the *y*-axis to the temperature, and the *z*-axis to the relative intensity (Fig. 8). To visualize events such as diffraction line shifts or growth and collapse of phases more precisely, a contour map in two dimensions was also projected from the 3D plot (Fig. 7). In the figure, the existence of phase domains is clearly highlighted by their contour lines (curves along which the diffracted intensity has a constant value). Fig. 7 is comparable with a topographic map used in cartography. The interval between lines is the difference in intensity between successive contour lines. When the lines are close together the magnitude of the gradient is large.

Using the mentioned two-dimensional diagram, 2θ–temperature (Fig. 7), it can be confirmed the existence of all these compounds together with their precise evolution as the temperature increases. In the region of 2θ between 60 and 76° it has not been possible to identify any compound due to the presence and overlapping of the peaks of the niobium sample holder.

At low temperatures it can be observed the decomposition of the hydromagnesite which takes place precisely at 275 °C. According to their thermal behavior, their total decomposition did not take place up to 600 °C, however it has not been possible to identify a intermediate phases through diffraction experiments during this range of temperature. This means that once the hydromagnesite has lost its crystallization water it loses completely its characteristic structure. Due to the overlapping of the characteristic diffraction peaks of the periclase with those of the niobium furnace, the formation of this phase, which comes from the decomposition of the hydromagnesite, could not be followed by means of the present experiment setup with this technique.

The total decomposition of the kaolinite to metakaolinite has taken place approximately at 600 °C, while the talc is the last starting material that decomposes. The talc peaks remain up to 700 °C, showing that its complete decomposition does not take place below this temperature. By means of the analysis of the three-dimensional diagram (Fig. 8), the temperature of decomposition of talc can be determined to be around 900 °C. This temperature agrees with the loss of the constitutional water molecules of the talc, therefore loss of its structure.

The evolution of the quartz it can be studied through the diffracted peak placed at 44° (Fig. 7). Between 500 °C and 600 °C it was observed the transformation of the α phase to the β quartz, by a displacement of the peak to smaller angles. This fact coincides with the reported temperature for this transformation at 573 °C [29].

After the decomposition of all the starting materials, the formation of an intermediate phase identified as μ-cordierite can be observed in the three-dimensional diagram (Fig. 8). This phase appears to an approximate temperature of 915 °C. Later on this disappears completely at 1030 °C.

In regard to mullite, this phase crystallizes during the first steps, coming from the decomposition of the metakaolinite. More precisely it begins to appear at 950 °C, having its maximum intensity at 1120 °C.

At higher temperatures, 1050 °C, it can be observed the protoenstatite crystallization and as the temperature increases, around 1120 °C, the cristobalite crystallization, coming from the amorphous silica produced as the result of the decomposition of talc and kaolinite as mentioned previously.

The spinel formation can be followed by means of the diffraction peak positioned at 76° (Fig. 7), which begins to appear around 1140 °C. Lastly at temperatures near 1200 °C the appearance of the cordierite is observed, confirming the results obtained by De Aza et al. [30], who observed that using the same

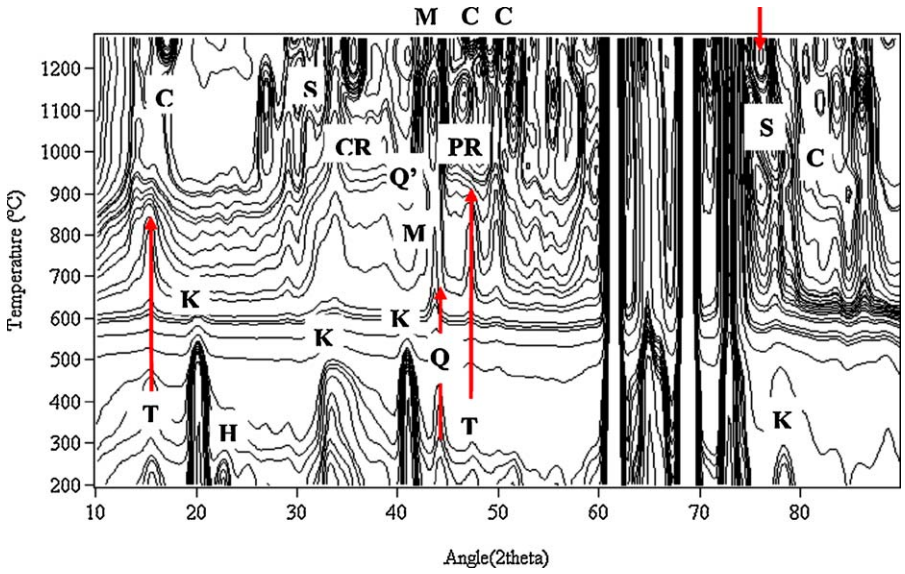

Fig. 7. Neutron Diffraction data: Contour map in two dimensions (2θ *vs.* temperature) projected from the 3D plot of Fig. 8. In the figure, the existence of phase domains is clearly highlighted by their contour lines (curves along which the diffracted intensity has a constant value). This figure is comparable with a topographic map used in cartography. H – hydromagnesite, K – kaolinite, T – talc, M – mullite, PR – protoenstatite, C – β-cordierite, S – spinel, CR – cristobalite, Q – α-quartz, Q' – β-quartz.

starting materials, the temperature of formation of the cordierite is around 1175 °C.

Referring to the β-quartz, it can be observed in the three-dimensional diagram (Fig. 8) that their intensity remains constant until approximately 1170 °C, when it begins to disappear. Stevens et al. [31] have demonstrated that the quartz could pass to cristobalite, through an intermediate phase that can be formed at a temperature higher than 1300 °C. Through this intermediate phase, β-quartz, it becomes cristobalite. Since in the present study the temperature limit has been of 1300 °C, the β-quartz remains without reacting. Its tendency to disappear is due to its dissolution in the amorphous phase, as they have already argued in some previous studies [20]. Its disappearance is also confirmed by the XRD data (Fig. 6).

3.3. Discussion of reaction mechanism

Bearing in mind all data obtained by XRD and ND it was thus possible to propose a justified mechanism that elucidates between the reactions leading to the cordierite synthesis and those that gave rise to the undesired phases generated during this process. To explain this mechanism, it has been considered that in solid state it is always more probable the reaction between two compounds than among three. Due to this, the cordierite formation ($2MgO{\cdot}2Al_2O_3{\cdot}5SiO_2$) will take place starting from the reaction of two binary compounds, or the reaction of an oxide and a binary compound. As natural raw materials have been used, the presence of small amount of impurities can lead to the presence of a small amount of glassy phase, but considering the

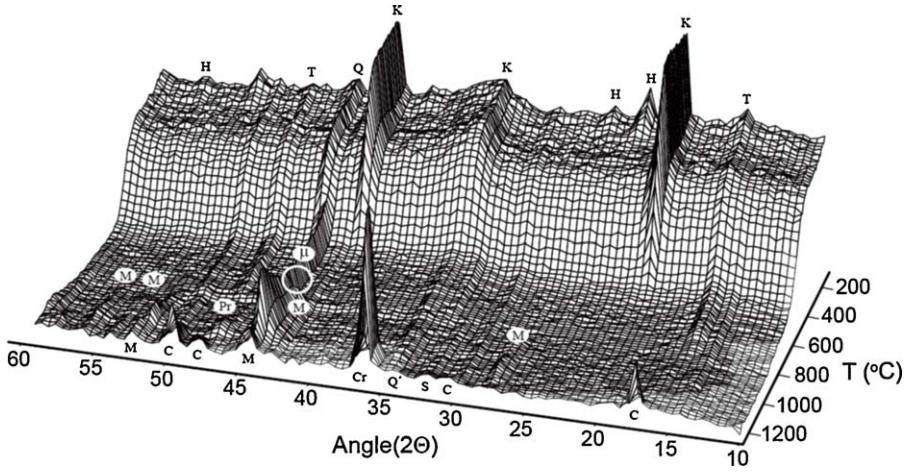

Fig. 8. Sequence of neutron diffracted patterns in a pseudo-3D fashion in which the *x*-axis corresponds to the diffraction angle 2θ, the *y*-axis to the temperature, and the *z*-axis to the relative intensity. T – talc, K – kaolinite, H – hydromagnesite, Q – α-quartz, μ – μ-cordierite, M – mullite, PR – protoenstatite, C – cordierite, S – spinel, Q' – β-quartz, CR – cristobalite.

obtained results, its presence is not significant and then it will be not considered.

In the two-dimensional diagram (Fig. 7) it can be clearly observed the decrease of the intensities of the peaks of the protoenstatite ($MgO{\cdot}SiO_2$) and mullite ($3Al_2O_3{\cdot}2SiO_2$) that takes place at the same time. It happens just at 1150 °C, stating that both compounds react to form cordierite (phase β) and spinel ($MgO{\cdot}Al_2O_3$), which is one of the impurities accompanying the cordierite. The reaction is the following:

$$3(MgO{\cdot}SiO_2) + 3Al_2O_3{\cdot}2SiO_2 \rightarrow 2MgO{\cdot}2Al_2O_3{\cdot}5SiO_2 + MgO{\cdot}Al_2O_3 \quad (1150\,^{\circ}C) \tag{1}$$

This reaction justifies the cordierite appearance starting from 1200 °C but not the formation of spinel at lower temperatures. Spinel can be detected at 1000 °C by XRD.

Additionally, it is necessary to know the role that the periclase (MgO) plays during the process. As mentioned previously the evolution of this phase, which comes from the decomposition of the hydromagnesite, could not be followed by means of the present Neutron Diffraction experiment setup due to the overlapping of the characteristic diffraction peaks of the periclase with those of the niobium furnace. Anyway, keeping in mind the results obtained from XRD experiments a reaction has been postulated. The periclase completely disappears at temperatures higher than 1200 °C. On the other hand, in the two-dimensional diagram (Fig. 7) it can be observed that at 1180 °C the protoenstatite's diffracted peaks have totally disappeared indicating that reaction (1) has already finished. However the decrease of the intensities of the peaks of the mullite continues at this temperature. Theses facts suggest that the mullite reacts with the periclase to form cordierite and spinel according to:

$$5(3Al_2O_3{\cdot}2SiO_2) + 15MgO \rightarrow 2(2MgO{\cdot}2Al_2O_3{\cdot}5SiO_2) + 11(MgO{\cdot}Al_2O_3) \quad (1118\,^{\circ}C) \tag{2}$$

(1) and (2) are the main reactions that explain the mechanism of formation of the cordierite. However there are still two phenomena without explanation:

(i) At 1200 °C there is still unreacted mullite. Since very pure reagents have been used, this fact is not attributable to the existence of secondary reactions that form mullite, but rather to requirement of a temperature higher than 1300 °C for its complete disappearance. On the other hand, as mentioned previously, the disappearance of the protoenstatite is clear at 1180 °C, indicating that reaction (1) has already finished. These facts imply that a small percentage of periclase (non-detectable by XRD) is still unreacted and coexist with the mullite at 1200 °C.

(ii) The presence of μ-cordierite can be observed looking over the diffraction pattern at 1000 °C. Sumi et al. [32,33] argued that the formation of this cordierite's phase is due to the reaction between metakaolinite and periclase. In Fig. 9 the ND integrated intensity of the main peak of this phase has been represented as a function of temperature. This phase appears between 915 °C and 1030 °C, starting to decrease above 975 °C. Since the formation of this phase takes place before the crystallization of the mullite, it can be affirmed that this phase is formed starting from periclase and metakaolinite following the reaction:

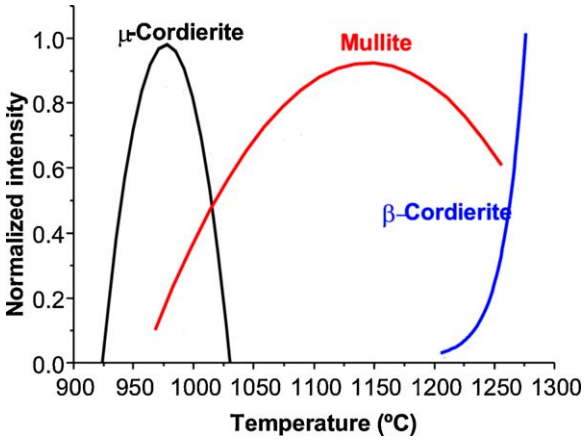

Fig. 9. Normalized intensity of the phases: μ-cordierite, mullite and β-cordierite *vs.* temperature. Neutron diffraction data.

$$5(Al_2O_3{\cdot}2SiO_2) + 5MgO \rightarrow 2(\mu\text{-}2MgO{\cdot}2Al_2O_3{\cdot}5SiO_2) + MgO{\cdot}Al_2O_3\,(915\,^{\circ}C) \tag{3}$$

The formation of this phase comes accompanied with the formation of the spinel. Therefore, it was not possible to follow its evolution by the neutron diffraction data due to the background generated and the overlapping of peaks. However this fact explains the early formation of the spinel detected by XRD at 1000 °C (Fig. 6). This phase stops to be formed just when the metakaolinite transform into mullite (975 °C). Also at this temperature the spinel begins to react causing its disappearance.

Different authors have observed that the cordierite μ-phase transforms to the β-phase when the homogeneity of amorphous phase is low [10,34]. Other studies, however, suggest that the μ-cordierite transforms into α-cordierite by a reaction with spinel [17]. In the present work it was observed that the intensities of the spinel's peaks keep on growing as the temperature increases (Fig. 7). Therefore is not probable that the cordierite reacts with spinel. These facts lead to the conclusion that this phase has transformed to the β-phase, which has not well-crystallized before reaching 1200 °C (Fig. 9).

4. Conclusions

The mechanism of cordierite synthesis has been studied using Neutron Diffraction (ND) with a high temperature furnace placed on the way of neutrons beam in order to obtain time resolved results of the reactions in this complex system. Thus, the complex reaction mechanism has been elucidated, discriminating the reactions prevailing at different temperatures, not only by inference (conventional XRD) but also by real time observation (ND).

The synthesis of cordierite from natural starting materials takes place through a complex mechanism. Depending on the

reactants used these reactions are different. The present paper presents results obtained during the cordierite synthesis starting from talc, kaolin and hydromagnesite. The reactions that take place are the following ones:

- Metakaolinite + periclase → μ-cordierite + spinel $T \approx 915\,^{\circ}C$
- Protoenstatite + mullite → β-cordierite + spinel $T \approx 1150\,^{\circ}C$
- Mullite + periclasa → β-cordierite + spinel $T \approx 1180\,^{\circ}C$
- μ-Cordierite → β-cordierite $T \approx 1200\,^{\circ}C$

This is the first time that the presence of the μ-cordierite phase has been observed when the synthesis is carried out in solid state from non-submicronic natural starting materials.

At the end of the entire process of synthesis, that involves several reactions, the obtained cordierite is always accompanied by a secondary phase, which is the spinel.

Acknowledgements

This work was supported by Science and Technology Inter-Ministry Commission of Spain under project MAT2010-17753.

Prof. Salvador de Aza passed away peacefully on 13 April 2011. Salvador was born on November 13, 1933. He devoted his life to his family, friends, and his love of researching and teaching. As a researcher and educator, he gave his time, energy and love to his students and faculty and research colleagues. His generosity and loving spirit will be missed by his family and friends.

References

[1]. Schreyer W, Schairer JF. Composition and structural states of anhydrous Mg-cordierites: a re-investigation of the system $MgO–Al_2O_3–SiO_2$. *J Petrol* 1961;**2**:324–406.
[2]. Granados EG. Degradación de materiales de cordierite en atmósferas de combustión. Doctoral Thesis, Universidad Carlos III, Madrid; 2002.
[3]. Karkhanavala MD, Hummel FA. The polymorphism of cordierite. *J Am Ceram Soc* 1953;**36**:389–92.
[4]. Meagher EP, Gibbs GV. The polymorphism of cordierite II. The crystal structure of indialite. *Can Miner* 1997;**15**:43–9.
[5]. Miyashiro A. Cordierite–indialite relations. *Am J Sci* 1957;**235**:43–62.
[6]. Menchi AM, Scian AN. Mechanism of cordierite formation obtained by the sol–gel technique. *Mater Lett* 2005;**59**:2664–7.
[7]. Fyfe CA, Gobbi GC, Putnis A. Elucidation of the mechanism and kinetics of the Si, Al ordering process in synthetic magnesium cordierite by ^{29}Si magic angle spinning NMR spectroscopy. *J Am Chem Soc* 1986;**108**:3218–23.
[8]. Predecki P, Hass J, Faber Jr J, Hitterman RL. Structural aspects of the lattice thermal expansion of hexagonal cordierite. *J Am Ceram Soc* 1987;**70**:175–82.
[9]. Miyashiro A, Hyama T, Yamasaki M, Miyashiro T. The polymorphism of cordierite and indialite. *Am J Sci* 1955;**253**:185–208.
[10]. Sei T, Eto K, Tsuchiya T. The role of boron in low-temperature synthesis of indialite (α-$Mg_2Al_4Si_5O_{18}$) by sol–gel process. *J Mater Sci* 1997;**32**:3013–9.
[11]. De Aza S, Espinosa de los Monteros J. Materiales cerámicos de cordierite. *Bol Soc Esp Ceram* 1967;**6**:731–44.
[12]. Tamborenea S, Masón AD, Aglietti EF. Mechanochemical activation of minerals on the cordierite synthesis. *Thermochim Acta* 2004;**411**:219–24.
[13]. Nakahara M, Kondo Y, Hamano K. Effect of talc grain size on microstructure of cordierite ceramics. *J Ceram Soc Jpn* 1995;**103**:1041–5.
[14]. Sampathkumar NN, Umarji AM, Chandrasekhar BK. Synthesis of α-cordierite (indialite) from fly ash. *Mater Res Bull* 1995;**30**:1107–14.
[15]. Goren R, Gocmez H, Ozgur C. Synthesis of cordierite powder from talc, diatomite and alumina. *Ceram Int* 2006;**32**:407–9.
[16]. Goren R, Ozgur C, Gocmez H. The preparation of cordierite from talc, fly ash, fused silica and alumina mixtures. *Ceram Int* 2006;**32**:53–6.
[17]. Naskar MK, Chatterjee M. A novel process for the synthesis of cordierite ($Mg_2Al_4Si_5O_{18}$) powders from rice husk ash and other sources of silica and their comparative study. *J Eur Ceram Soc* 2004;**24**:3499–508.
[18]. Acimovic Z, Pavlovic L, Trumbulovic L, Andric L, Stamatovic M. Synthesis and characterization of the cordierite ceramics from non-standard raw materials for application in foundry. *Mater Lett* 2003;**57**:2651–6.
[19]. Karagedov G, Feltz A, Neidnicht B. Preparation of cordierite ceramics by sol–gel technique. *J Mater Sci* 1991;**26**:6396–400.
[20]. Tulyaganov DU, Tukhtaev ME, Escalanate JI, Ribero MJ, Labrincha JA. Processing of cordierite based ceramics from alkaline–earth–aluminosilicate glass, kaolin, alumina and magnesite. *J Eur Ceram Soc* 2002;**22**:1775–82.
[21]. de Aza AH, Rodríguez MA, Rodríguez JL, de Aza S, Pena P, Convert P, Hansen T, Turrillas X. Decomposition of dolomite monitored by neutron thermodifractometry. *J Am Ceram Soc* 2002;**85**(4):881–8.
[22]. Turrillas X, Mas-Guindal MJ, Hansen TC, Rodríguez MA. The thermal explosion synthesis of AlNi monitored by neutron thermodiffractometry. *Acta Mater* 2010;**58**:2769–77.
[23]. Copley JRD. *The fundamentals of neutron powder diffraction: practice guide*. National Institute of Standards and Technology, Special publications EEUU; 2001. p. 960–2.
[24]. Brunauer G, Frey F, Boysen H, Schneider H. High temperature thermal expansion of mullite: an in situ neutron diffraction study up to 1600 °C. *J Eur Ceram Soc* 2001;**21**:2563–7.
[25]. ITT Visual Information Solutions, USA. *Program IDL version 5.2*; 1998.
[26]. Guinea JG, Frías JM. *Recursos minerales de España*. Madrid: Edt. Consejo Superior de Investigaciones Científicas; 2002.
[27]. Akao M, Maruno F, Iwai S. The crystal structure of hydromagnesite. *Acta Cryst* 1974;**B30**:2670–2.
[28]. Akao M, Iwai S. The hydrogen bonding of hydromagnesite. *Acta Cryst* 1977;**B33**:1273–5.
[29]. Sosman RB. *The phases of silica*. Rahway, NJ: The American Chemical Society, Quinn & Boden Company, Inc.; 1927.
[30]. de Aza S, Espinosa de los Monteros J. The mechanism of cordierite formation in ceramic bodies. In: *IV scientific technological conference of glass and ceramics*. 1972. p. 269–80.
[31]. Stevens SJ, Hand RJ, Sharp JH. Polymorphism of silica. *J Mater Sci* 1997;**32**:2929–35.
[32]. Sumi K, Kobayashi Y, Kato E. Synthesis and sintering of cordierite from ultrafine particles of magnesium hydroxide and kaolinite. *J Am Ceram Soc* 1998;**81**:1029–32.
[33]. Sumi K, Kobayashi Y, Kato E. Synthesis and sintering of cordierite from kaolinite and basic magnesium carbonate. *J Ceram Soc Jpn* 1998;**106**:91–5.
[34]. Selvaraj U, Komarneni S, Roy R. Synthesis of glass-like cordierite from metal alkoxides and characterization by Al-27 and Si-29 MASNMR. *J Am Ceram Soc* 1990;**73**:3663–9.